Electro-optical modulator in a polymer-infiltrated silicon slotted photonic crystal waveguide heterostructure resonator

Jan Hendrik Wülbern,[1,*] Alexander Petrov,[1] and Manfred Eich[1]

[1]*Technische Universität Hamburg-Harburg, E-12, Eissendorfer Str. 38, D-21073 Hamburg, Germany*
**Corresponding author: jan.wuelbern@tu-harburg.de*

Abstract: We present a novel concept of a compact, ultra fast electro-optic modulator, based on photonic crystal resonator structures that can be realized in two dimensional photonic crystal slabs of silicon as core material employing a nonlinear optical polymer as infiltration and cladding material. The novel concept is to combine a photonic crystal heterostructure cavity with a slotted defect waveguide. The photonic crystal lattice can be used as a distributed electrode for the application of a modulation signal. An electrical contact is hence provided while the optical wave is kept isolated from the lossy metal electrodes. Thereby, well known disadvantages of segmented electrode designs such as excessive scattering are avoided. The optical field enhancement in the slotted region increases the nonlinear interaction with an external electric field resulting in an envisaged switching voltage of approximately 1 V at modulation speeds up to 100 GHz.

OCIS codes: (130.0250) Optoelectronics; (130.4110) Modulators; (130.5296) Photonic crystal waveguides; (130.3120) Integrated optics devices; (230.5750) Resonators; (230.5298) Photonic crystals.

References and links

1. A. Shacham, K. Bergman, and L. P. Carloni, "On the Design of a Photonic Network-on-Chip," First International Symposium on Networks-on-Chip (IEEE, 2007) 53–64.
2. T. Asano, B. S. Song, Y. Akahane, and S. Noda, "Ultrahigh-Q nanocavities in two-dimensional photonic crystal slabs," IEEE J. Sel. Top. Quantum Electron. **12**, 1123–1134 (2006).
3. I. Park, H. S. Lee, H. J. Kim, K. M. Moon, S. G. Lee, B. H. O, S. G. Park, and E. H. Lee, "Photonic crystal power-splitter based on directional coupling," Opt. Express **12**, 3599–3604 (2004), http://www.opticsinfobase.org/oe/abstract.cfm?URI=oe-12-15-3599.
4. A. Y. Petrov and M. Eich, "Zero dispersion at small group velocities in photonic crystal waveguides," Appl. Phys. Lett. **85**, 4866–4868 (2004).
5. A. Y. Petrov and M. Eich, "Dispersion compensation with photonic crystal line-defect waveguides," IEEE J. Sel. Areas Commun. **23**, 1396–1401 (2005).
6. S. G. Johnson, P. R. Villeneuve, S. H. Fan, and J. D. Joannopoulos, "Linear waveguides in photonic-crystal slabs," Physical Review B **62**, 8212–8222 (2000).
7. B. Analui, D. Guckenberger, D. Kucharski, and A. Narasimba, "A fully integrated 20-Gb/s optoelectronic transceiver implemented in a standard 0.13-mu m CMOS SOI technology," IEEE J. Solid-State Circuits **41**, 2945–2955 (2006).
8. Y. A. Vlasov, M. O'Boyle, H. F. Hamann, and S. J. McNab, "Active control of slow light on a chip with photonic crystal waveguides," Nature **438**, 65–69 (2005).
9. M. Lipson, "Compact electro-optic modulator's on a silicon chip," IEEE J. Sel. Top. Quantum Electron. **12**, 1520–1526 (2006).
10. R. S. Jacobsen, K. N. Andersen, P. I. Borel, J. Fage-Pedersen, L. H. Frandsen, O. Hansen, M. Kristensen, A. V. Lavrinenko, G. Moulin, H. Ou, C. Peucheret, B. Zsigri, and A. Bjarklev, "Strained silicon as a new electro-optic material," Nature **441**, 199–202 (2006).
11. T. D. Kim, J. W. Kang, J. Luo, S. H. Jang, J. W. Ka, N. Tucker, J. B. Benedict, L. R. Dalton, T. Gray, R. M. Overney, D. H. Park, W. N. Herman, and A. K. Jen, "Ultralarge and Thermally Stable Electro-Optic Activities from Supramolecular Self-Assembled Molecular Glasses," J. Am. Chem. Soc. **129**, 488–489 (2007).

#103439 - $15.00 USD Received 7 Nov 2008; revised 23 Dec 2008; accepted 23 Dec 2008; published 2 Jan 2009

12. J. D. Luo, Y. J. Cheng, T. D. Kim, S. Hau, S. H. Jang, Z. W. Shi, X. H. Zhou, and A. K. Y. Jen, "Facile synthesis of highly efficient phenyltetraene-based nonlinear optical chromophores for electrooptics," Organic Lett. **8**, 1387–1390 (2006).
13. M. Lee, H. E. Katz, C. Erben, D. M. Gill, P. Gopalan, J. D. Heber, and D. J. McGee, "Broadband Modulation of Light by Using an Electro-Optic Polymer," Science **298**, 1401–1403 (2002).
14. J. H. Wülbern, M. Schmidt, M. Eich, U. Hübner, R. Boucher, F. Marlow, and W. Volksen, "Omnidirectional photonic band gap in polymer photonic crystal slabs," Appl. Phys. Lett. **91**, 221104 (2007).
15. C. Liguda, G. Bottger, A. Kuligk, R. Blum, M. Eich, H. Roth, J. Kunert, W. Morgenroth, H. Elsner, and H. G. Meyer, "Polymer photonic crystal slab waveguides," Appl. Phys. Lett. **78**, 2434–2436 (2001).
16. G. Bottger, C. Liguda, M. Schmidt, and M. Eich, "Improved transmission characteristics of moderate refractive index contrast photonic crystal slabs," Appl. Phys. Lett. **81**, 2517–2519 (2002).
17. M. Schmidt, M. Eich, U. Huebner, and R. Boucher, "Electro-optically tunable photonic crystals," Appl. Phys. Lett. **87**, 121110 (2005).
18. J. M. Brosi, C. Koos, L. C. Andreani, M. Waldow, J. Leuthold, and W. Freude, "High-speed low-voltage electro-optic modulator with a polymer-infiltrated silicon photonic crystal waveguide," Opt. Express **16**, 4177–4191 (2008), http://www.opticsinfobase.org/oe/abstract.cfm?URI=oe-16-6-4177.
19. T. Baehr-Jones, M. Hochberg, G. X. Wang, R. Lawson, Y. Liao, P. A. Sullivan, L. Dalton, A. K. Y. Jen, and A. Scherer, "Optical modulation and detection in slotted Silicon waveguides," Opt. Express **13**, 5216–5226 (2005), http://www.opticsinfobase.org/oe/abstract.cfm?URI=oe-13-14-5216.
20. V. R. Almeida, Q. F. Xu, C. A. Barrios, and M. Lipson, "Guiding and confining light in void nanostructure," Opt. Lett. **29**, 1209–1211 (2004).
21. A. Di Falco, L. O'Faolain, and T. F. Krauss, "Dispersion control and slow light in slotted photonic crystal waveguides," Appl. Phys. Lett. **92**, 83501 (2008).
22. T. Baehr-Jones, B. Penkov, J. Huang, P. Sullivan, J. Davies, J. Takayesu, J. Luo, T. D. Kim, L. Dalton, and A. Jen, "Nonlinear polymer-clad silicon slot waveguide modulator with a half wave voltage of 0.25 V," Appl. Phys. Lett. **92**, 163303 (2008).
23. Avaible at www.cst.com.
24. T. Yamamoto, M. Notomi, H. Taniyama, E. Kuramochi, Y. Yoshikawa, Y. Torii, and T. Kuga, "Design of a high-Q air-slot cavity based on a width-modulated line-defect in a photonic crystal slab," Opt. Express **16**, 13809–13817 (2008), http://www.opticsinfobase.org/oe/abstract.cfm?URI=oe-16-18-13809.
25. J. M. Lee, D. J. Kim, G. H. Kim, O. K. Kwon, K. J. Kim, and G. Kim, "Controlling temperature dependence of silicon waveguide using slot structure," Opt. Express **16**, 1645–1652 (2008).
26. J. P. Hugonin, P. Lalanne, T. P. White, and T. E. Krauss, "Coupling into slow-mode photonic crystal waveguides," Opt. Letters **32**, 2638–2640 (2007).
27. G. H. Kim, Y. H. Lee, A. Shinya, and M. Notomi, "Coupling of small, low-loss hexapole mode with photonic crystal slab waveguide mode," Opt. Express **12**, 6624–6631 (2004), http://www.opticsinfobase.org/oe/abstract.cfm?URI=oe-12-26-6624.
28. K. K. McLauchlan and S. T. Dunham, "Analysis of a compact modulator incorporating a hybrid silicon/electro-optic polymer waveguide," IEEE J. Sel. Top. Quantum Electron. **12**, 1455–1460 (2006).
29. D. Widman, H. Mader, and H. Friedrich, *Technology of integrated circuits* (Springer, 2000).
30. R. Soref and B. Bennett, "Electrooptical effects in silicon," IEEE J. Quantum Electron. **23**, 123–129 (1987).
31. R. Blum, M. Sprave, J. Sablotny, and M. Eich, "High-electric-field poling of nonlinear optical polymers," J. Opt. Soc. Am. B **15**, 318–328 (1998).
32. M. Eich, A. Sen, H. Looser, G. C. Bjorklund, J. D. Swalen, R. Twieg, and D. Y. Yoon, "Corona poling and real-time second-harmonic generation study of a novel covalently functionalized amorphous nonlinear optical polymer," J. Appl. Phys. **66**, 2559–2567 (1989).

1. Introduction

The strong research interest in micro photonics stems from the ever increasing demand for bandwidth in information processing on all levels. Long distance, high bandwidth communication is well established on the basis of lightwave technology. However, also on comparatively short and shortest distances the use of light as information carrier is becoming increasingly interesting as power consumption and latency times limit the feasible bandwidth achievable with electronics [1]. Therefore using micro photonic circuits for chip-to-chip and for on-chip communication will be essential to meet future demands on data rates and computing speeds. Key building blocks of micro photonics such as resonators, directional couplers, delay lines and dispersion compensators can be realized using photonic crystals (PhCs) slabs [2–5]. PhC slabs are implemented as an array of holes in a high index slab surrounded by a low index material providing confinement of light by total internal reflection [6].

Silicon is a widely used material for PhC slabs today due to its high refractive index (n = 3.5) and low absorption in the near infrared part of the spectrum, which allows excellent

#103439 - $15.00 USD Received 7 Nov 2008; revised 23 Dec 2008; accepted 23 Dec 2008; published 2 Jan 2009

optical confinement. Furthermore, with silicon on insulator (SOI) substrates, the material system is intrinsically compatible with CMOS electronics, allowing access to a mature manufacturing infrastructure and the ability to combine optical and electronic networks on a single chip [7]. An electro-optic (EO) modulator is a key building block for enabling interconnects of such on chip networks. Several types of modulators have been proposed in SOI structures based either on thermo-optic [8] effects or charge injection p+-i-n+ diode [9] configurations. The former is limited in its switching time to 0.1 μs [8] and the latter is intrinsically limited by the carrier life time, however, recently modulation of 10 Gb/s has been demonstrated [9].

The use of the Pockels effect for EO modulation based on electronic displacement polarization is desirable as it is inherently much faster than the effects described above. The Pockels effect is not present in native silicon due to its centrosymmetric crystal structure. This fact prohibits second order hyperpolarisability, which is a prerequisite for the Pockels effect. Recently, Jacobsen et al. demonstrated that the centrosymmetry of silicon can be broken by straining the crystal lattice, the achieved effect however, is comparatively small [10]. Polymers on the other hand offer very high Pockels coefficients (> 300 pm/V) [11, 12] and a purely electronic hyperpolarisability, which offers modulation speeds in excess of 150 GHz [13]. Polymers themselves only offer moderate refractive indices ($n \approx 1.6$) and a less developed nano-structuring fabrication technology compared to silicon. Recently, both PhC structures with a direction independent band gap for transverse electric (TE) polarization in hexagonal lattices [14] as well as EO modulation in PhCs have been demonstrated for polymer based PhC slabs [15–17]. However, the light confinement ability and realizable band gaps are small relative to high index materials.

Brosi et al. [18] discussed a concept to combine both material types to achieve high speed modulation in a PhC based Mach-Zehnder interferometer. Their concept uses silicon as core material surrounded by polymer replacing all air regions, including the infiltration of holes. The ability of EO active polymers to infiltrate structures on the scale of tens to hundreds of nanometers had been previously shown to work from solution [19]. To enhance the interaction of the external electric field and optical field in the nonlinear polymer region a slot was introduced into a slow light PhC defect waveguide. Such a slot on the scale of hundred nanometers is known to lead to an enhancement of a perpendicularly polarized optical field (i.e. TE polarization) in the slot region, due to the discontinuity of the refractive index and the merging of the evanescent tails of the mode inside the polymer region [20, 21]. Recently Baehr-Jones et al. used this field enhancement in an EO-polymer filled slotted silicon waveguide to achieve electro-optic modulation in a classical Mach-Zehnder geometry, with a rather large geometric footprint (arm lengths of 2 cm) [22].

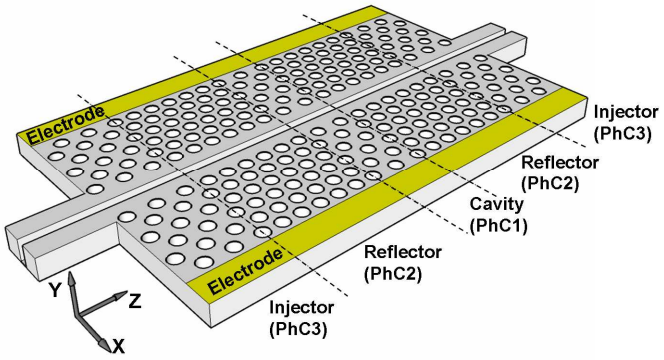

Fig. 1. Schematic of the proposed slotted PhC waveguide heterostructure modulator. The resonator is defined by the cavity region (PhC1) and the reflector (PhC2), in plane light confined is achieved by the mode gap effect. To facilitate coupling to the cavity an injector section (PhC3) between PhC2 and the slotted ridge waveguide is designed. The stripe electrodes are placed alongside the PhC waveguide.

#103439 - $15.00 USD Received 7 Nov 2008; revised 23 Dec 2008; accepted 23 Dec 2008; published 2 Jan 2009

Our novel concept of an electro-optic modulator is schematically presented in Fig. 1. We envision a resonant cavity design to achieve large modulation depths and at the same time maintaining an ultra compact geometrical footprint. Both aspects are optimally accounted for in a heterostructure type photonic crystal cavity, as these devices have the highest reported Q values with a minimal modal volume [2]. The heterostructure is formed by joining PhC waveguides with slightly different lattice constants. The cavity section (PhC1) has a larger lattice constant compared to the reflector section (PhC2). By creating a heterostructure cavity using a slotted PhC waveguide filled with a nonlinear optical (NLO) polymer it is possible to shift the position of the resonance peak in the frequency spectrum via modulation of the refractive index of the NLO polymer by means of an external electric field.

This article is organized as follows; in section 2.1 we first consider an isolated slotted heterostructure cavity of silicon embedded in polymer to investigate and optimize its intrinsic quality factor. In section 2.2 we add access waveguides to the structure to study the transmission behavior of the device. We add and optimize an injector section to the device to decrease its insertion loss. In the third section we show that variations of the refractive index in the slotted region due to the Pockels effect can shift the resonance frequency of the device, thus allowing its operation as an EO modulator.

2. Slotted hybrid PhC heterostructure cavity

2.1. Unloaded resonator performance

We first consider the design and performance of the unloaded PhC heterostructure resonator, i.e. without access waveguides. In Fig. 2 we show the band structure of a slotted PhC waveguide of silicon ($n_{Si} = 3.5$) embedded in polymer material ($n_{Poly} = 1.6$). The geometry parameters are chosen to be: lattice constant $a = 410nm$, radius $r = 0.3a$, waveguide width $W = 1.4\sqrt{3}a$, slot width $W_{slot} = 150nm$ and slab thickness $d_{Si} = 220nm$. The parameters were chosen to obtain a defect mode at the center of the photonic band gap and considerable field enhancement in the slotted region (inset Fig. 1(a)). A narrower slot would create an even stronger enhancement of the electric field; however we chose the above value to facilitate processability of the device.

By slightly increasing the lattice constant in propagation direction of the waveguide the defect mode is shifted to lower frequencies, thus creating a mode gap (Fig. 2(a)). We use this mode gap to form a heterostructure resonator by elongating the lattice constant in a two lattice constant long cavity section of the slotted PhC waveguide. Optical fields with frequencies within the mode gap will be trapped in this cavity region. Obviously, choosing a larger step of the lattice constant will result in a larger mode gap. We were interested to see how the resonant behavior, namely the Q factor is affected by the difference in lattice constant of cavity and reflector.

Three dimensional numerical simulations using CST Microwave Studio [23], which is based on the finite integration technique (FIT), were performed to calculate resonant behavior and field distributions. For all simulations we chose meshings with discretization fine enough such that further detailing did not improve the quality of the results considerably (mesh size was typically $\lambda_{mat}/10$). The simulation volume was chosen to be 25 lattice constants lateral and 50 lattice constants along the defect waveguide. We compared the intrinsic Q of such a cavity and the penetration depth, which is the 1/e value of the optical field strength, in propagation direction of the electric field into the reflector section. The lattice constant in the cavity region a_1 was increased in 5nm steps, the results are summarized in Fig. 2(b). The largest Q of 3.7×10^5 is obtained for the smallest elongation of $\Delta a = 5nm$. However, this geometry also exhibits the largest penetration depth, which implies the necessity of a longer reflector section and thus increasing the device footprint.

#103439 - $15.00 USD Received 7 Nov 2008; revised 23 Dec 2008; accepted 23 Dec 2008; published 2 Jan 2009

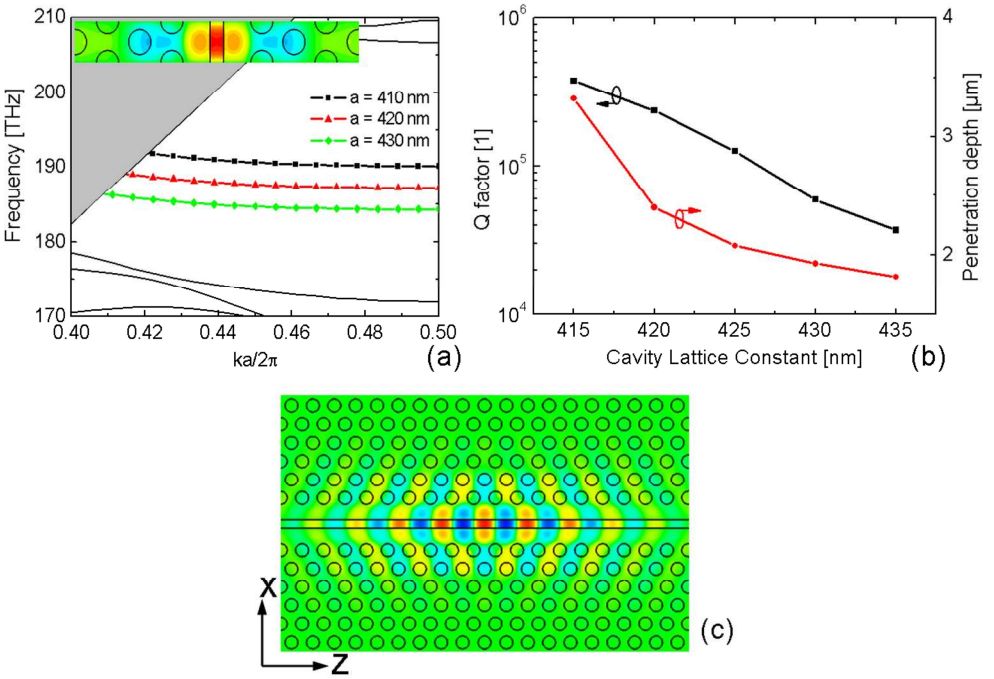

Fig. 2. (a) Defect mode of the slotted PhC waveguide, the inset shows the field distribution of the defect mode in the x-z-plane. (b) Intrinsic quality factor and penetration depth in the reflector section of the PhC heterostructure resonator as a function of cavity lattice constant. (c) shows the field distribution of the resonant mode.

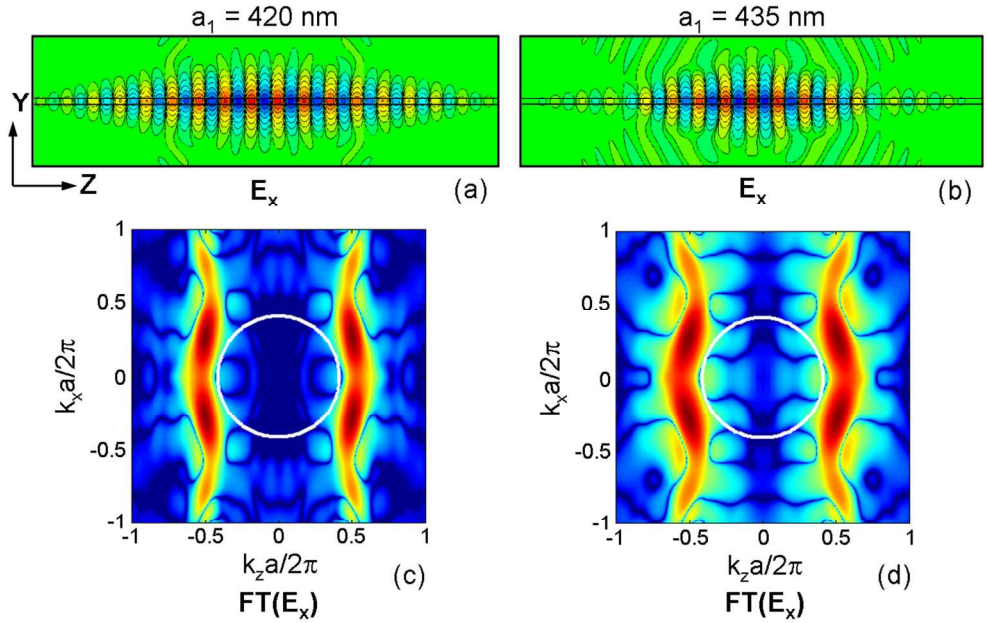

Fig. 3. (a) and (b) show the real space field distribution of the E_x component at $x = 0$ in logarithmic scale. Enhanced vertical scattering at larger cavity lattice constant a_1 can be observed. (c) and (d) show the k-space field distribution of the same field vector component at $y = 0$ in false color representation of identical scale. For wave vectors inside the white circle the total internal reflection condition is violated.

#103439 - $15.00 USD Received 7 Nov 2008; revised 23 Dec 2008; accepted 23 Dec 2008; published 2 Jan 2009

A reduction in the intrinsic Q factor of a PhC cavity implies an increase in vertical losses due to out of plane scattering. In the field distribution in the y-z-plane presented in Fig. 3(a) and (b) this effect is clearly observable. A larger step in lattice constant leads to an envelope of the electric field function stronger deviating from Gaussian shape and consequently results in a decreased quality factor as explained by Asano et al. [2]. To study this behavior we performed two dimensional spatial Fourier transforms of the electric field distribution of the cavity mode (Fig. 3(c) and (d)). The white circles in the field plots indicate the leaky region into the polymer cladding ($k = n_{Poly} 2\pi / \lambda_0$). For wave vector components within these regions (light cones) the total internal reflection condition is not satisfied. These can serve as escape routes for the optical energy and are responsible for out of plane scattering. It can be seen that the lower Q heterostructures show stronger k-vector components within the light cones.

These results clearly indicate a trade-off between high Q and low penetration depth, i.e. device size, when choosing the cavity lattice constant. At the same time a trade-off results for the free spectral range of the device and the achievable Q. The free spectral range is predisposed by the mode gap width, which itself is determined by the difference in cavity lattice constant. If a larger free spectral range is desired then a longer cavity lattice constant should be chosen, however at the expense of a reduced Q. For our device and the remainder of this article we consider a cavity lattice constant of $a_1 = 420nm$. This results in a free spectral range of approximately 25 nm.

The Q factors reported here turned out to be about a factor of 4 smaller compared to the slotted heterostructures reported in [24]. This is not surprising, since the cladding material here is polymer as opposed to air and leads to larger leaky region. Consequently more wave vector components are inside the light cone, due to the reduced refractive index contrast between cladding and core material. However, as discussed in more detail in section 2.2, this is not a disadvantage for the envisaged electro-optical modulation device as Q-values well above 10^4 would curb switching speeds unacceptably.

A common problem in silicon photonic devices is the temperature dependence of the transmission behavior, due to the thermo-optic effect of silicon. However, at the same time the thermo-optic coefficients of silicon and polymers are typically of different sign. Since in a slotted waveguide design most of the optical field is concentrated in the slot and thus in the polymer, the opposing thermo-optic effect of the polymer can be used to minimize or even eliminate the temperature dependence of the device for a given operating point. This has been shown for slotted ring resonator devices [25].

In our case the frequency shift is about 7 GHz/K, if only the thermo-optic effect of the silicon ($dn/dt = -1.8 \times 10^{-4}\ K^{-1}$) is considered. A resonator with a quality factor of 10^4 would be shifted by its full width half maximum (FWHM) at a temperature difference of $\Delta T = 27K$ only. Even a simple temperature control should be able to stabilize the temperature well within this margin. To even increase the allowable operating temperature range of the resonator a proper optimization of the geometry is needed taking into account the polymer filling as explained in [25]. This will be addressed in a subsequent publication.

2.2. Loaded resonator performance

To operate the proposed device in transmission, slotted ridge waveguides are added as shown in Fig. 1. We chose a cavity with $a_1 = 420$ nm and reflector section with length $N_2 = 8a$. In our simulations we found that simply butt coupling the ridge waveguide to the PhC heterostructure waveguide results in a very high insertion loss of the device at resonance of more than -16 dB. To mitigate these insertion losses we introduced an injector section (PhC3) of just four lattice constants in length between the reflector section and the ridge waveguide. In a first step, the lattice constant of this transition section was chosen to be the same as the lattice constant of the cavity region (PhC1), allowing optical waves at the resonance frequency to propagate in this region. This increased the transmission to approximately -8 dB. We reason that by first coupling to a Bloch mode of the PhC waveguide, optical tunneling

#103439 - $15.00 USD Received 7 Nov 2008; revised 23 Dec 2008; accepted 23 Dec 2008; published 2 Jan 2009

through the reflector region to the cavity region is facilitated, which results in less out of plane scattering and hence the maximum transmission of the resonator is increased.

However, at the resonance frequency the defect mode of PhC1 and PhC3 is in the slow light regime (Fig. 4), which causes back reflections at the interface from ridge to PhC waveguide due to the group velocity and thus group refractive index mismatch of the waveguides [26]. In a second step, to compensate for this effect, we chose PhC3 with a lattice constant of $a_3 = 450nm$, thereby shifting the defect mode in the fast light regime at the resonance frequency (Fig. 4). We then saw a significantly increased transmission at resonance to roughly -3 dB from initially -8 dB. This shows that the theory presented in [26] for standard PhC waveguides can also be applied to slotted PhC waveguides to enhance the light injection efficiency and thereby the transmission performance. Note that a transition section of just four lattice constants is sufficient to achieve this improvement. It is desirable to keep this section as short as possible, not only to keep the geometric footprint of the device small, but also to avoid significant radiation losses from PhC 3 due to operation above the light line.

Naturally, in a coupled system as considered here, the total (or loaded) Q factor and maximum transmission at resonance depend on the intrinsic Q of the cavity and the coupling strength of the system. The former we considered in the previous section and the latter is controlled by the length of the reflector region PhC2. When increasing the length of this region, the reflectivity of PhC2 and the total Q of the device are increased, while the maximum transmission is decreased. Analytically this is expressed by the following relations [27]:

$$\frac{1}{Q_{total}} = \frac{1}{Q_{vertical}} + \frac{1}{Q_{horizontal}}, \tag{1}$$

and

$$T_{\max} = \left(\frac{Q_{total}}{Q_{horizontal}} \right)^2 = \left(1 - \frac{Q_{total}}{Q_{vertical}} \right)^2, \tag{2}$$

where horizontal and vertical Q factor represent the in plane and out of plane energy decay respectively. The vertical Q is comparable to the intrinsic or unloaded Q of the cavity and the horizontal Q increases with an increasing length of the reflector section PhC2.

From (2) it is therefore clear that at a given intrinsic (or vertical) Q the maximum transmission has to decrease with increasing total Q. Hence, to compare the effect of the optimized transition section we performed device simulations for various lengths ($N_2 = 8…14$) of the reflector section PhC2 and plotted the obtained maximum transmission values versus the total Q (Fig. 4(b)). We clearly see a significant improvement in transmission at any given total Q with the transition section PhC3 in place with $a_3 = 450nm$

For the operation as an electro-optic modulator we can limit ourselves to Q factors of about 10^4, since the Q factor is directly proportional to the photon lifetime τ inside the resonant cavity and its resonant frequency ω_0 ($Q = \omega_0 \tau$). This results in an upper limit to the modulation frequency of the device given by $f_Q = \tau^{-1}$. This result emphasizes that for modulation purposes the Q factor of a cavity should not exceed 10^4 if a bandwidth of the order of 100 GHz is desired. From Fig. 4 we see that Q values in this order of magnitude would result in a transmission of approximately -3 dB.

#103439 - $15.00 USD Received 7 Nov 2008; revised 23 Dec 2008; accepted 23 Dec 2008; published 2 Jan 2009

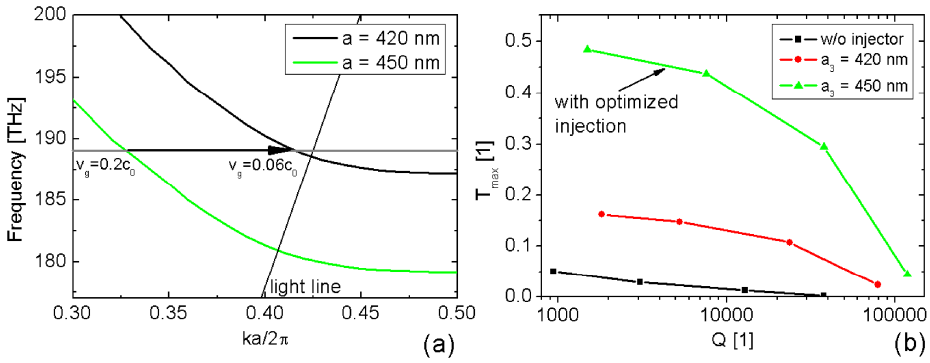

Fig. 4. (a) 3D band diagram of the slotted PhC waveguide defect mode. By choosing a larger lattice constant the light at the resonance frequency (ω_{res}) is first coupled to a fast light mode of the transition section PhC 3 and then excites into the slow light mode of the cavity. The fast light region of the transition section is above the light cone, however, this section has a very short length of just $4a_3$. (b) Maximum transmission vs. Q factor cavities with and without an injector section, reflector length is varied between 8 and 14 lattice constants.

3. Electro-optic modulation

Figure 5 shows how the transmission spectrum shifts when changing the refractive index in the slotted region of the PhC heterostructure cavity (reflector length N_2 = 10, Q = 8000). A refractive index change of just $\Delta n = 0.001$ results in a wavelength red shift of approximately $\Delta\lambda = 0.12$ nm. This strong sensitivity is a result of the optical field enhancement in the slotted region (Fig. 2). The change in refractive index due to an applied electric modulation field E is given by the relation $\Delta n = n_{Poly}^3 r_{33} E/2$, where $E = V/W_{slot}$ with slot width W_{slot}, applied voltage V, Pockels coefficient r_{33} and the polymer refractive index n_{Poly}. To compare resonant modulator devices typically the full width half maximum voltage V_{FWHM} is used [28], which corresponds to the voltage needed to shift the resonance by its spectral width at half maximum intensity. By choosing a state of the art polymer material with r_{33} = 150 pm/V [11, 12] and using the relations given above we calculate V_{FWHM} = 0.8 V with a quality factor Q = 8000.

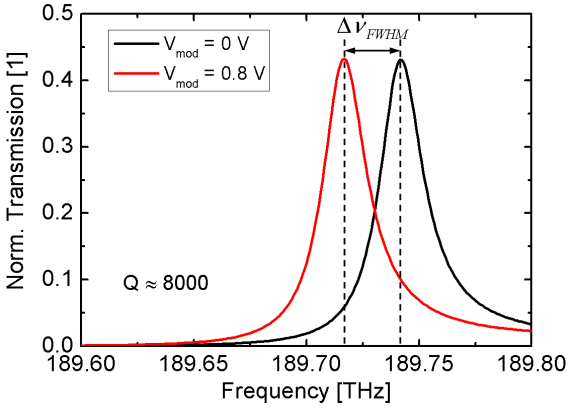

Fig. 5. Calculated resonance spectra of heterostructure cavity in a silicon/polymer hybrid PhC slab at electro-optically shifted refractive indices of the polymer slot material. The voltage required to shift the spectrum by the spectral width of the resonance is V_{FWHM} = 0.8 V when using an electro-optically active polymer with r_{33} = 150 pm/V. The slight asymmetric shape of the spectrum is a consequence of the close spectral proximity of the mode gap edge at higher frequencies.

#103439 - $15.00 USD Received 7 Nov 2008; revised 23 Dec 2008; accepted 23 Dec 2008; published 2 Jan 2009

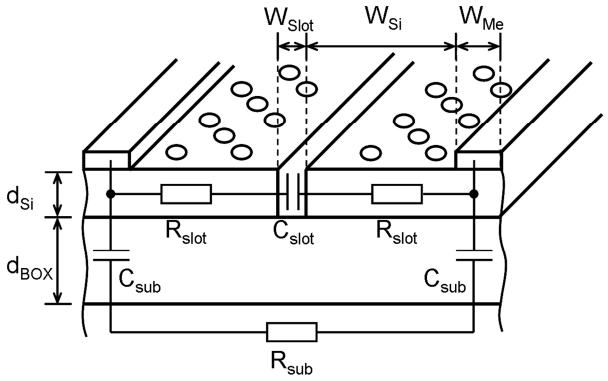

Fig. 6. Sketch of the electrically relevant geometry of the device.

To apply an electrical modulation signal to the slot, metal electrodes are deposited laterally to the defect waveguide in a distance W_{Si}, as indicated in Fig. 1. The PhC in this design offers the two fold functionality of being optically isolating and electrically conducting at the same time, thus allowing the modulation field to be applied to the electro-optical polymer inside the slotted region while keeping the optical field from reaching the contacting metal electrodes and introducing additional losses. By choosing W_{Si} = 3 µm (roughly 8 lattice constants in ΓM direction) the optical loss from the metal contacts is negligible, as the optical field is by 40 dB lower at this point compared to the exit port of the device. Due to the ultra compact dimensions of the device the maximum modulation frequency is not limited by the group velocity mismatch of the electrical and optical wave, as it is usually the case in macroscopic traveling wave modulator configurations. In our case the bandwidth limit is dictated by the charging time needed to load the capacitance C_{slot} formed by the slot through the ohmic resistance R_{slot} across the silicon due to the finite silicon resistivity. Since the device dimensions are small compared to the RF wavelengths, the electrical behavior can be modeled by lumped elements. The charging time is given by $\tau = 2R_{slot}C_{slot}$ which yields the 3 dB frequency $f_{3dB} = 1/(2\pi \cdot 2R_{slot}C_{slot})$, with the resistance $R_{slot} \approx W_{Si}\rho / Fd_{Si}l$ and capacitance $C_{slot} = \varepsilon_0 n_{poly}^2 d_{Si} l / W_{slot}$ (for the definition of variables see Fig. 6), where ρ is the resistivity of the used silicon, l the device length and $F = 0.67$ is the fill factor. R is increased by this factor due to the reduced conducting material in the PhC volume, as, compared to silicon, the polymer filled regions have a near zero conductivity. The formula for the resistance is only a first order approximation, as the exact value of a perforated material is not easily calculated. The silicon resistance is approximated using a fill factor approach for estimating the effect of perforation. As a modulation frequency of f_{3dB} = 100 GHz is desired and using the geometry values given above we arrive at a minimum resistivity of about 0.1 Ωcm, which can be achieved by using a dopant concentration of $n_D = 10^{17}$ [29]. At this relatively modest doping level the additional optical loss of ~2 dB/cm [30] in the bulk silicon is negligible considering the device length of about 10 µm.

As indicated in Fig. 6, apart from the $R_{slot}C_{slot}$ circuit of the slotted PhC waveguide, a parasitic shunt $R_{sub}C_{sub}$ circuit through the substrate is also present in this device. These parasitic elements induce a capacitive coupling to the substrate and hence an additional loss mechanism, which might increase the power consumption of the device. To estimate these losses we compare the current through each RC arm of the electrical circuit, which is inversely proportional to its impedance. The substrate capacitance is given by $C_{Sub} = \varepsilon_0 n_{poly}^2 l(W_{Si} + W_{Me}) / d_{BOX}$, where $d_{BOX} = 2\mu m$ is the separation of SOI layer and silicon substrate and the width of the metal electrodes W_{Me} is assumed to be equal to W_{Si}.

#103439 - $15.00 USD Received 7 Nov 2008; revised 23 Dec 2008; accepted 23 Dec 2008; published 2 Jan 2009

The series connection of the two substrate capacitances then turns out to be comparable to the capacitance of the slot ($\frac{1}{2} C_{Sub} \approx C_{slot}$). The silicon substrate is assumed to have the same resistivity as the SOI layer. Since this layer is orders of magnitude thicker than the top waveguiding layer, the substrate resistance R_{sub} is much smaller than R_{slot}. From this consideration it is clear that the impedance presented by the parasitic circuit is mostly capacitive and hence consumes primarily reactive power. This of course has to be considered in the design of the feeding lines in order to match the load impedance to the generator.

The exact design of the electrical coupling to this device and the RF-power needed is currently under investigation and, as it represents the external driving circuitry, will be addressed in a subsequent publication. However, we would like to point out here, that this parasitic $R_{sub}C_{sub}$ shunt element does not limit the performance of the modulator at the envisioned operation frequency of 100 GHz, as it does not have an impact on the time constant of the $R_{slot}C_{slot}$ element presented by the slotted PhC waveguide. We have verified this by rigorous FIT simulations. Observing the electrical field strength in the slot at 100 GHz shows that it has dropped to roughly 70% of the DC case, which corresponds to 3dB. This is in good agreement with the results obtained from the lumped element considerations of the $R_{slot}C_{slot}$ element and at the same time this confirms the vanishing effect of the parasitic $R_{sub}C_{sub}$ shunt element on the bandwidth.

In order to observe the Pockels effect in polymeric materials, a non-centrosymmetric orientation of the chromophore ensemble is required. Such an anisotropic molecular arrangement is achieved by poling [31] of the polymer infiltrating the slot. While applying a sufficiently high DC electric field to the slot (~ 100 V/μm), employing the same electrodes as used for the RF modulation, the sample is heated to the glass transition temperature of the polymer. At this temperature the chromophore molecules are aligned along the field lines of the applied electric field. This field is maintained while the sample is cooled down to room temperature, thereby freezing the molecular orientation of the chromophores [32].

4. Summary and conclusion

In summary we presented a novel design of an ultra compact resonant modulator structure based on a heterostructure cavity formed in a slotted PhC waveguide infiltrated with an electro-optically active polymer material. We showed that vertical scattering can be reduced by appropriately choosing the lattice constant in the cavity region and hence cavities with high intrinsic Q factors can be designed. By introducing an injector section with fast light propagation we optimized the coupling to the resonator and significantly enhanced the maximum transmission at resonance. The proposed geometry is extremely sensitive to refractive index changes in the slot region, which in combination with state of the art polymer materials is capable of modulation with voltages of just 0.8 V and frequencies up to 100 GHz. The achieved Q factor is suitable for high bandwidth modulations.

Acknowledgments

This research is supported by the German Research Foundation (DFG). The authors acknowledge the support from CST, Darmstadt, Germany with their Microwave Studio software. We thank Martin Jenett for useful discussions.

#103439 - $15.00 USD Received 7 Nov 2008; revised 23 Dec 2008; accepted 23 Dec 2008; published 2 Jan 2009